Impact of Chemical Impurities on the Crystalline Cement Clinker Phases Determined by Atomistic Simulations

Hegoi Manzano,[*,†] Engin Durgun,[*,‡] Mohammed Javad Abdolhosseine Qomi,[†] Franz-Josef Ulm,[†] Roland. J. M. Pellenq,[†] and Jeffrey. C. Grossman[‡]

[†]Department of Civil and Environmental Engineering and [‡]Department of Materials Science and Engineering, Massachusetts Institute of Technology, Cambridge, Massachusetts 02139, United States

Ⓢ *Supporting Information*

ABSTRACT: The presence of chemical substitutions is believed to play a crucial role in the hydration reactions, structure, and elastic properties of cement clinker phases. Hence, substitutions are of great technological interest, as more efficient production of cement clinkers would result in a reduction of CO_2 emissions, as well as possible economic benefits. Here we use a combination of classical and quantum mechanical simulation methods to study the detailed physicochemical changes of the clinker phases alite (Ca_3SiO_5) and belite (Ca_2SiO_4) when Mg^{2+}, Al^{3+} and Fe^{3+} guest ions are incorporated into their structure. Using classical force field methods, we considered random substitutions among possible sites and different compositions in order to identify the preferential substitution sites on the crystalline structures. Then, the resulting structural changes that take place to accommodate the guest ions are investigated and discussed in detail. Using quantum mechanical density functional theory calculations the electronic structure of representative configurations has been computed to determine the potential impact of impurities on the reactivity.
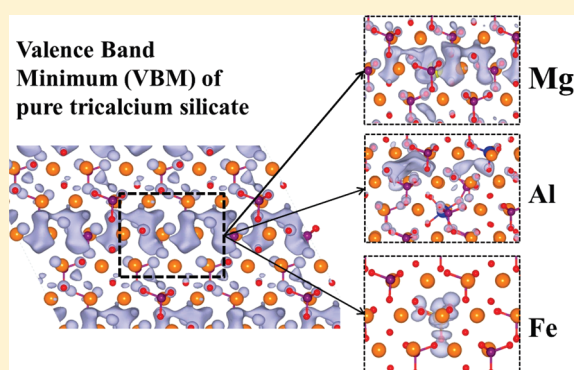
INTRODUCTION

Cement is the most utilized material in the world. It is a highly versatile material, with remarkable mechanical properties and chemical durability. However, concomitant to these positive attributes is the massive quantity of CO_2 emitted during its manufacturing, accounting for roughly 5% of global anthropogenic carbon dioxide emissions.[1] Researchers have long pursued modifications to the manufacturing process that would allow for a decrease in cement's environmental footprint. Examination of the phase diagram of calcium and silicon oxides reveals a straightforward way of achieving this objective, namely, the use of belite (dicalcium silicate) instead of alite (tricalcium silicate) as the main clinker phase. The temperature necessary to produce belite is ~1200C, while alite requires temperatures of 1500.[2] Clearly, the reduction of the required energy to form belite would entail both economic and environmental benefits. Unfortunately, the strength development is much slower in belitic cements, rendering them essentially useless in construction. The search for a form of belite with higher reactivity has been carried out by a trial and for many decades. Several strategies have been attempted, for example, modifying the chemical structure of belite by thermal processing[3−5] or including chemical impurities.[3−5] Regarding the latter, and despite partial success,[6] there is little control or understanding of where the atomic substitutions take place, their effect on the structure, and their role on the chemical reactions. Although little used to date in this field, atomistic simulation

techniques could be a critical tool to overcome the aforementioned difficulties, as they allow one to determine the position of chemical impurities and examine the resulting properties on the clinker. To this end, in the present work we use a combination of force field and density functional theory methods to study the impact of the most common chemical substitutions in alite and belite, and suggest appropriate routes to modify their reactivity.

Alite is the main component of Portland cement, accounting for 70 wt %. It is a chemically modified form of pure tricalcium silicate (Ca_3SiO_5 or C_3S), which exhibits a set of reversible phase transitions upon heating.[7−12] The crystal structures of the different alite polymorphs are similar, consisting of independent SiO_4^{4-} tetrahedra and three ionic sites: one O^{2-} and two Ca^{2+} positions[13] (see figure 1). The polymorphs differ in the orientation of the SiO_4^{4} tetrahedra, which affects the symmetry and the coordination of the Ca and O atoms.[14,15] In this study we choose the alite M3 polymorph refined from a single crystal by Mumme et al.,[16,17] since it is the most abundant polymorph in cement clinkers.[8] The most common substitutions are those of Mg^{2+} for Ca^{2+}, but $2 \times Al^{3+}$ or $2 \times Fe^{3+}$ for $Ca^{2+} + Si^{4+}$ also take place.[9] The role of the substitutions as stabilizers of the monoclinic phases and their solubility limits in alite have been extensively
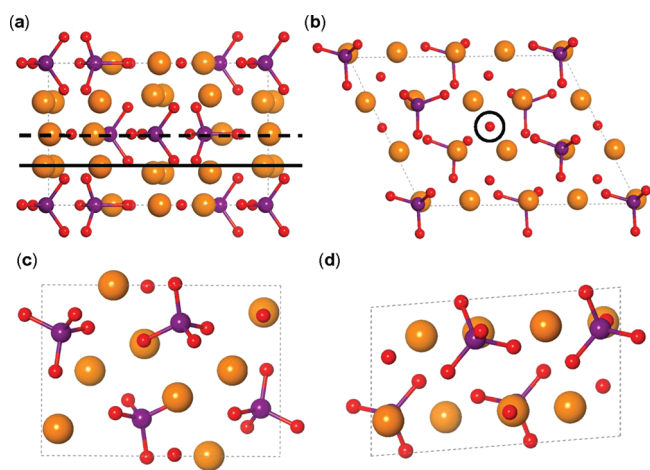
Figure 1. Representation of the alite MIII polytype and β-belite crystalline structures. (a) alite {001} plane projection, (b) alite {010} plane projection, (c) belite {001} plane projection, and (d) belite {010} plane projection. Calcium silicon and oxygen atoms are represented as orange purple medium-sized and red spheres, respectively. Silicon−oxygen bonds are shown to represent the strong covalent bond, forming the SiO_4^{4-} silicate groups. In the figure the structural features of alite mentioned in the text are shown: (a) lines to indicate the flexible and rigid planes, and (b) a circle around the free oxygen atom.

Table 1. Number of Simulations Performed for Each Chemical Substitution and Substitution Amount[a]

	alite				belite			
%	Mg	Al	Fe	%	Mg	Al	Fe	total
0.5	40			1	20			
1	40	50	50	2	20	25	25	
1.5	100			3	50			
2	100	100	100	4	50	50	50	
2.5	100			5	50			
3	100	100	100	6	50	50	50	
total	480	250	250		240	125	125	1470

[a] The substitution percentages are within the limit values experimentally observed in ordinary Portland clinker cements[1,9].

studied[7,14,18−20] (see table 1). Stephan and co-workers[21] found by Xray diffraction experiments a slight decrease in the cell parameters for the M1 polytype of synthetic alite with Mg^{2+}, Al^{3+}, and Fe^{3+} incorporations. They evaluated also the effect of these substitutions on the hydration reaction, and found that Mg^{2+} does not change the hydration speed while Al^{3+} enhances it slightly and Fe^{3+} decreases it.[21] The results agree in general with other studies.[22]

Belite is the second phase of importance in ordinary Portland cement. Similar to alite, belite is a chemically modified form of dicalcium silicate (Ca_2SiO_4 or C_2S), and presents a sequence of reversible polymorphs with temperature.[1,9,12,23] The crystal structure of belite is composed of SiO_4^{4-} tetrahedra and Ca^{2+} ions, differing from alite in the absence of the ionic O^{2-} ions (see Figure 1). The α_H, α_L, and β polymorphs are derived from the α form by a decrease of the symmetry because of the disorder of SiO_4^{4-} groups and slight changes in the positions of the Ca atoms.[23−26] We chose the beta polymorph of belite for the present study as it is by far the main one observed experimentally in ordinary Portland cement clinker.[23,27−29] In belite, the most important incorporation of guest ions is that of Al and Fe atoms, while the replacement of Ca by Mg is less important than in alite. The limiting values of the incorporations, presented in table 1, and the stabilization effect on the high temperature polymorphs have been studied in detail.[23,25,26,29,30] Surprisingly, despite the interest in belite as a crucial component for an environmentally friendly concrete,[31] current information regarding the guest ion effect on the crystalline cell parameters or reactivity is severely limited. Concerning the reactivity, the hydration rate of belite has been reported to be equal or even greater when Al^{3+} is introduced, and decrease considerably when Fe^{3+} is the guest ion.[29] The hydration rate decreases as well when the incorporation of iron amount increases.[29,32]

Despite the fact that atomistic simulation methods have demonstrated great potential in material science research,[33] they

have been scarcely used for studies of the cement clinker. The first study was done by Feng and co-workers,[24] who used a simple cluster model to study the bond length and atomic charges of β and γ belite by ab initio methods. More recently, Manzano et al. calculated the elastic and electronic properties of tricalcium aluminate by density functional theory (DFT),[34] and suggested the active site blockage as the flash setting retardation mechanism. In this work a combination of force field and DFT calculations is employed to identify the effect of Mg^{2+}, Al^{3+}, and Fe^{3+} incorporation on the structure, elasticity, and reactivity of the clinker phases alite and belite. Using the force field calculations, different incorporation amounts in random positions were simulated to determine the most stable substitutions sites, structural changes and resulting elastic behavior. Snapshots of the most probable configurations were then used in the more computationally expensive DFT calculations, to study their reactivity by examining the electronic structure of the crystals. Our results are in good agreement with existing experimental data, and help to understand the detailed effects of impurities on the clinker crystal properties in great at the atomic scale.

■ METHODOLOGY

Force Field Simulations. In our force field calculations, we employed the so-called core−shell potential model, which have been previously tested for calcium silicate[35,36] and calcium aluminoferrite[37] crystals. Detailed information regarding the potential functional forms and parameters are given in the Supporting Information. The simulations were performed using the GULP code.[38,39] The crystalline structures were optimized by relaxing the unit cell parameters and the atomic positions. Symmetries were eliminated once the supercell was generated to allow for anisotropic variations of the lattice vectors. To accelerate the convergence of the Coulombic energy, the Ewald summation method was chosen[40] with a real space cutoff radius of 8 Å. The search for local minima was carried out by the Newton−Raphson algorithm, updating the Hessian each ten steps using the Broyden−Fletcher−Goldfarb−Shannon (BFGS) scheme.[41,42] The convergence tolerances for the forces and energies during the relaxation were 10^{-5} eV/Å^2 and 10^{-3} eV, respectively.

Starting from the pure crystals, we made random substitutions, replacing directly atom by atom without any a priori rules or modification of the lattice parameters or other input quantities. The studied substitutions include the most common cationic and mixed cationic−anionic substitutions, which are Mg^{2+} for Ca^{2+} and $2Al^{3+}$ or $2Fe^{3+}$ for $Ca^{2+}+Si^{4+}$. In all cases, the unit cell charge remained neutral. Substitutions up to several percent were considered in a supercell of
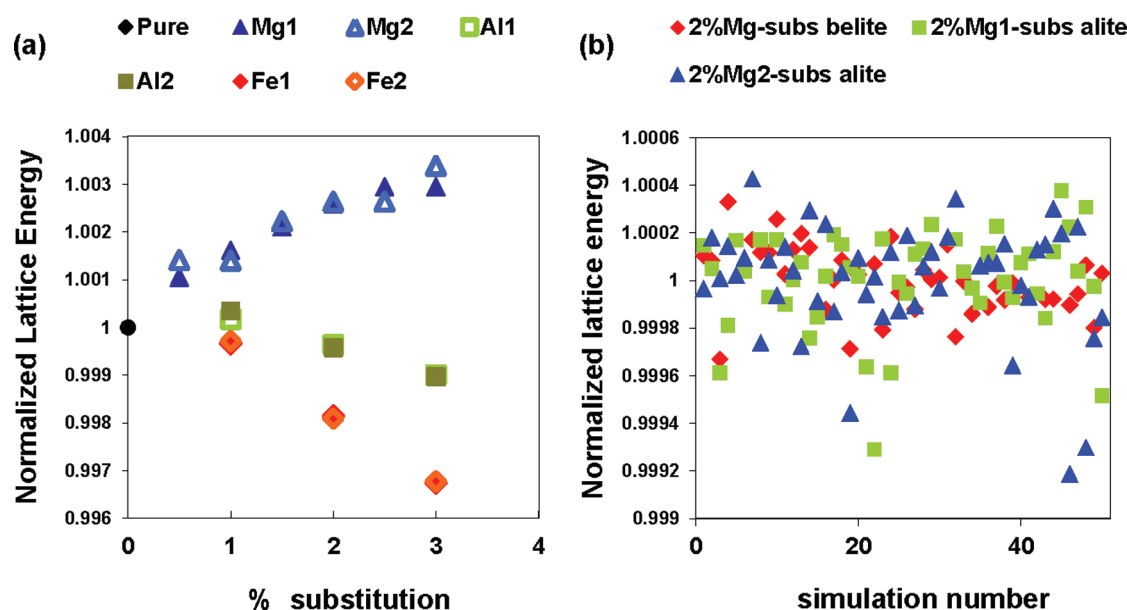
B

dx.doi.org/10.1021/cg200212c |*Cryst. Growth Des.* XXXX, XXX, 000−000

Figure 2. (a) Normalized lattice energy (eV) of alite as a function of the substitution percent for Mg^{2+}, Al^{3+}, and Fe^{3+}. The number together with the element in the legend represents the two possible calcium sites, that in the Ca—O—Ca layer (Ca1) and that in the Ca—O—Si layer (Ca2), see the text for details. The normalizing factor is the energy of the crystal without impurities. (b) Normalized lattice energy values for 50 random simulations with 2% Ca^{2+} by Mg^{2+} substitutions in alite and belite. The normalizing factor is the average energy of the 2% Mg^{2+} substituted crystal. Note that the normalization values in parts a and b are different.

$2 \times 2 \times 2$, in accord with the experimentally reported data of the limit of incorporation and usual values found in the ordinary Portland cement clinker.[1,9] These percentages are shown in Table 1, together with the number of random replacements for each composition. This combinatorial approach gives us a sample large enough to consider the averages as statistically significant. The simulations that did not reach convergence or had ill-defined values in the elastic constants (identified by Poisson coefficients negative or bigger than 0.5) were eliminated from the sampling.

Density Functional Theory Simulations. The force field methods allow us to study the structural and energetic properties in a rapid and relatively accurate way, although electrons are not taken into account explicitly. On the contrary, although at a much high computational cost, density functional theory calculations provide the necessary insight on the electronic structure to study the effect of substitutions on alite and belite reactivity. Snapshots from our force field simulations are used for the density functional theory calculations performed using the VASP simulation package.[43] We used Projected Augmented Wave[44] (PAW) potentials including Ca $3s^2$, $3p^64s^2$; O $2s^22p^4$; Mg $2p^63s^2$; Al $3s^23p^1$; and Fe $3d^74s^1$ electrons as valence states and a plane wave basis set energy cutoff of 500 eV. The exchange-correlation potential was approximated within the PBE Generalized Gradient Approximation (GGA).[45] Integration over the Brioullin zone was performed at the gamma point. The structure was relaxed within DFT using the conjugate gradient method, with simultaneous minimization of the total energy and interatomic forces. The convergence on energy and the maximum residual force allowed on each atom were set to 10^{-5} eV and 10^{-2} eV/Å² respectively.

■ RESULTS AND DISCUSSION

Substitution Site. The first question we address is which sites would be most favorable for substitution, since experimental techniques are not able to resolve the exact location of the guest ions. In the case of the Mg^{2+} by Ca^{2+} replacement in alite, it was

suggested that the Ca—O—Ca plane would be a preferential location, as the higher flexibility in the cation-oxygen distance would allow a better rearrangement to fit the smaller magnesium atom.[16] These features can be easily distinguished in Figure 1a where a plane of Ca—O—Si atoms marked with a dashed line, and the second one to a Ca—Ca (or Ca—O—Ca if preferred) marked by a plain line. To our knowledge nothing has been suggested regarding substitution sites of Al and Fe, as the effect of a double substitution in a calcium and silicon positions is more difficult to predict. In Figure 2 we present the average alite lattice energy with Mg^{2+} Al^{3+} and Fe^{3+} incorporation in site 1 (close symbols) and site 2 (open symbols) for different substitution percentages. The notation used throughout the rest of the paper is X1 for the substitutions in the Ca—O—Ca layer and X2 for those in the Ca—O—Si layer, where X is the guest ion. The standard deviations around the mean energy values are lower than 0.05% in all cases. It can be seen in Figure 2a that for each substitution type and percentage the mean value is similar independent of the Ca that was replaced, which clearly indicates that there is no preferential substitution in any of the calcium sites for any of the oxide substitutions. In belite this structural feature does not exist, all the calcium sites have similar environments, and so no comparison between different crystallographic sites was performed. Nevertheless, a comparison of the energy values for simulations of random substitutions performed for a given chemical substitution and percentage in alite and belite is shown in Figure 2b. The plot illustrates the spread in the energy when diverse crystalline positions are substituted. Similar patterns, or the absence of a pattern to be more precise, where found for aluminum and iron. Despite the existence of some preferential substitution sites, we did not found any trend on the energy with the volume, density, cell parameters, or distance between

C

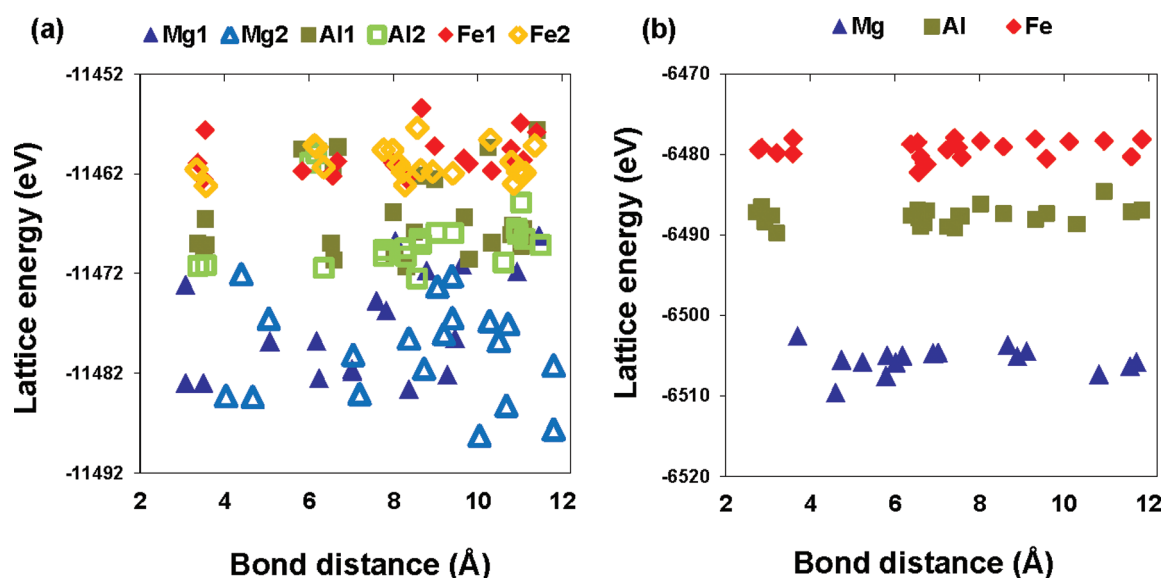dx.doi.org/10.1021/cg200212c |*Cryst. Growth Des.* XXXX, XXX, 000–000

Figure 3. Total lattice energy in eV as a function of the distance between guest ions for (a) alite and (b) belite.

impurities. This conclusion is supported by our DFT calculation, in which we could not find any pattern for the energy of the substituted crystals.

Once we determine that there is no preferential site for the chemical substitution, the next question we address is the distribution of the guest ions in the material. A plot of our computed lattice energies versus guest ion distances is presented in figure 3 for the three substitution types. As can be seen in the figure there is no energy trend for the Ca^{2+} by Mg^{2+} replacement, which means that the substituted sites could be, at least thermodynamically, in any position within the unit cell, no matter how close or far from another chemical defect. This result is perhaps expected, as the elements are isovalent and the charge distribution at the cation site and surrounding oxygen atoms is not expected to change much. The main effect upon substitution is the atomic size variation between Ca and Mg, and the trend we observed could be expected. However, in the case of Al^{3+} and Fe^{3+} the substitution is aliovalent, and local charge defects are created. Nonetheless, we can see in figure 3 that the stability of the structures does not depend on the distance between substituted sites. This result suggests that any combination of sites is equally probable, as the guest ions do not stabilize each other, and oxygen atoms are responsible for the charge balance. This picture might change if other substitutions which entail a mixed cation—anion substitution are investigated, as suggested in ref 46.

Atomic Structure Rearrangement. Since neither the lattice sites nor the distance between chemical defects impact the stability of the crystal, we seek a different structural feature that might correlate in lower lattice energies with particular substitution site combinations. The answer lies in the rearrangement of the silicate tetrahedra. In figure 4 it can be seen how the perfectly ordered arrangement of the SiO_4^{4-} groups changes when Mg^{2+} ions are included in alite (more examples for the rest of the guest ions in alite and belite are given in the Supporting Information). Experimentally it has been determined that disorder in the silicate tetrahedral orientation exists and that it affects the calcium ion coordination.[13,47,48] In the present calculations, we do not find a correlation between the substitution sites and
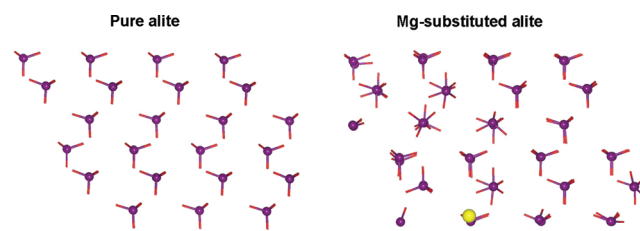

Figure 4. Example of silicate tetrahedral orientation in pure alite and substituted with magnesium. For a better view, the calcium and oxygen atoms were eliminated from the picture. The silicate tetrahedra are represented by the sticks linked to the atoms, which represent the Si—O bonds. Mg is represented as a yellow sphere.

the silicate tetrahedral orientation. However, the reorganization could be the reason for the stability, since an optimal reorientation can more easily accommodate the guest ions, balancing the charge and dissimilar cation sizes, leading to a more stable structure. It is interesting to note that silicate tetrahedra far from the defect site are also distorted, not just those close to it. We can think of the rearrangement as a "pulling mechanism", in which the disorder of some tetrahedra close to the defect induces changes in their neighbors, expanding a certain degree of disorder to further sites. Note that since the charges are fixed in our force field approach, the only way of counterbalancing the charge is by spatial movements, so our simulations may overestimate the atomic rearrangement. However, our DFT calculations confirm such distortion albeit to a lesser extent, as do experimental XRay diffraction results.[13,47]

The induced disorder in the structure impacts on the bond distances in the material, as can be observed in the partial radial pair distribution function, $g_{X-O}(r)$ (with X = Ca, Si, Mg, Al, and Fe). We focused on the first peak, corresponding to the first coordination shell, which includes only the oxygen atoms forming the SiO_4^{4-} group, and oxygen atoms up to 3.3 Å, for Al, Fe and Ca cations, as one oxygen atom located at this large distance is sometimes included in the first coordination shell of alite and belite.[9] The Ca—O and Si—O radial pair distributions for alite
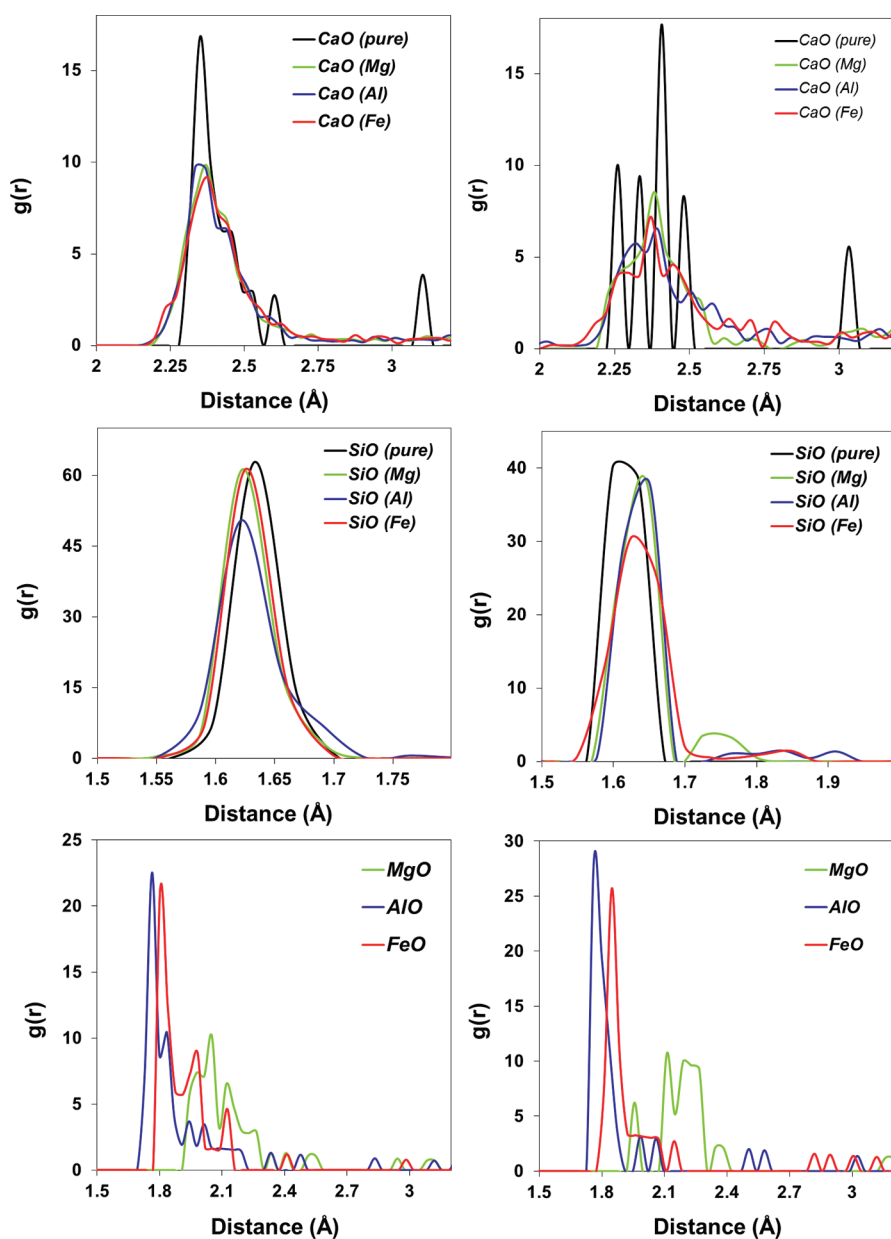
Figure 5. Calcium—Oxygen partial radial pair distribution functions g(r) in substituted alite (left) and belite (right). At larger distances the radial pair distribution function converges properly to 1, though we focused here in the first peak.

and belite with 4 substitutions per unit cell are presented in figure 5. The first conclusion that we can draw from the $g_{X-O}(r)$ plot is that the Ca—O coordination polyhedral is deformed when guest ions are incorporated into the crystals, while the Si—O distances are nearly unaffected. The Ca—O correlation at distances larger than 3 Å is completely lost, and the sharp bond distribution of the pure crystal is deformed into a more variable bond length distribution. The bond strength of ionic calcium—oxygen bonds make them more susceptible to deformations than the covalent silicon—oxygen bonds. Therefore, the defect balancing mechanism can be viewed as a reorientation of the silicate tetrahedra (which conserve their shape) to counterbalance the charge and size of the defects, inducing a movement and small distortion of the calcium coordination polyhedra. As can be seen in Figure 5, the effect of all the guest ions is similar for the rearrangement of alite and belite. The main difference between

the two crystals is that the silicate tetrahedra are unaltered in alite, while in belite some oxygen atoms have larger bond lengths than the average 1.64 Å. This difference might arise from the absence of the ionic oxygen in belite, which gives enough flexibility in alite to make unnecessary the distortion of any Si—O bonds. The partial radial pair distribution of Mg—O, in figures 5d and 5f for alite and belite, respectively, clearly shows a shorter bond length than that of Ca—O, due to the atomic size, but in the same range. In the case of Al^{3+} and Fe^{3+} substitutions, it is interesting to note that $g_{X-O}(r)$ is closer to that of silicon—oxygen rather than a mixture between the Si—O and Ca—O profiles, which indicates a preference for the tetrahedral environment. These guest ions might induce more disorder than Mg^{2+}, which is expected due to the difference in valence configurations for the substitutions, although the impact on the structural and elastic properties is similar, as we discuss. It
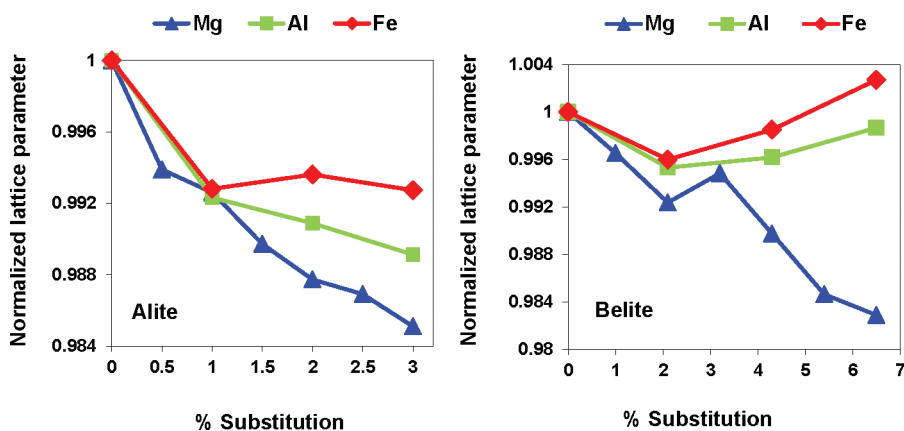
Figure 6. Evolution of alite and belite lattice parameters as a function of the chemical substitution percentage, averaged over all the substitution types. The results for each substitution and lattice parameter is given independently in the Supporting Information.

must be mentioned that the tetrahedral preference is confirmed by our DFT calculations.

Crystalline Unit Cell. We have this far established that the positions of the chemical defects are random in the unit cell, and that silicate tetrahedral rearrangement is the stabilization mechanism. Now we turn to evaluate the impact of the impurities on the crystalline structure and properties. In Figure 6, we present the unit cell volume evolution of the crystals as a function of substitution percentage for each guest ion. Comparison of the different substitutions shows that the level of change in the volume follows the expected ordering with element size, $Mg^{2+} > Al^{3+} > Fe^{3+}$, where the bigger the ions, the lower the decrease on the unit cell volume, in agreement with the bond-length bond-strength relationships discussed previously. Several studies have shown that incorporation of Mg^{2+}, up to about the 3%, decreases the unit cell of alite.[49] The exact values cannot be directly compared because of the coexistence of T1 and M3 polymorphs in the experiment, but the volume decreases about 0.9%, in good agreement with our calculations. In belite, we also observe a decrease of the volume by up to 3% with guest ion incorporation. However, as we reach higher guess ion incorporation, the unit cell volume reaches a minimum and starts increasing for Al^{3+} and Fe^{3+}, but not for Mg^{2+}. The effect arises from the double substitution that involves Ca and Si, rather than Ca alone. The Ca^{2+} ion has a larger ionic radius than any of the studied guest elements, but when the silicate monomer is part of the substitution, both the aluminate and ferrite tetrahedra are bigger, and hence the volume increase at large substitution percentages. A similar effect was found for Al^{3+} substituted alite: when the substitution included both calcium and silicon the unit cell decreased, while if only the calcium by aluminum replacement was involved the unit cell increased.[50]

More detailed information about the evolution of each lattice parameter is given in the Supporting Information. For alite, our calculations reproduce the trend experimentally observed by Stephan et al.[21] that the change in the lattice parameters can be tracked solely by following two cell lengths. In their case, they studied a synthetic M1 polymorph, and the varying sides were b, c, while in our M3 variant the evolving parameters are a, b. In general, the a and b cell vectors decrease as the substitution amount increases for all the elements, while the c vector fluctuates. Nevertheless, the variation in the unit cell parameters

is almost negligible, only 0.8%, in good agreement with the experimental data.[21]

The changes in belite lattice parameters upon substitution are more pronounced. The a and b lattice vectors increase while c decreases. The main change takes place in the β angle, decreasing from 94° to 90°, which might indicate a transition from the β to polymorph. It is difficult to distinguish whether this is a force field limitation from or a real phase transition, due to the similarity between both polymorphs. According to the experimental data, the amount of guest ions needed to stabilize the alpha form is higher than for the beta form. We could expect then a change for higher substitution percentages, rather than over the entire range. However, since the optimization procedure can only bring us to the local minima of energy, the structural similarity could make the alpha polymorph more accessible than the beta one in our simulations. In order to explore further the complex belite polymorphism and stabilization of higher temperature (and more reactive) polymorphs, we plan to study the polymorphic transitions with temperature by atomistic simulations in the near future.

Our DFT calculations indicate trends similar to the force field results for alite. The lattice parameters tend to decrease a little less than in the force field simulations (0.4%) in excellent agreement with the literature.[21] In the case of belite, the DFT unit cell sides also follow the force field trends, although more scattered results than in alite are obtained. We did not observe changes larger than 0.8 degrees in the beta angle; in other words, there is no phase transition upon doping within the substitution percentages studied. The mismatch might arise from the different simulation methodologies: as metinoned earlier the fixed charges in the force field might make necessary a higher distortion of the unit cell to accommodate defects than in density functional theory calculations. Nevertheless, due to the minor discrepancy we do not expect significant changes in the discussed atomic sites, silicate tetrahedral rearrangement, and elastic properties.

Elastic Properties. We next explore the changes in the elastic properties upon chemical substitution by computing the indentation modulus (M), as it is the most common parameter for measuring elastic properties of cement paste components.[51] A derivation of the indentation modulus calculation is given in the Supporting Information. The evolution of our computed indentation modulus with the substitution amount in alite and belite are presented in Figure 7. For both phases, it is clear that M
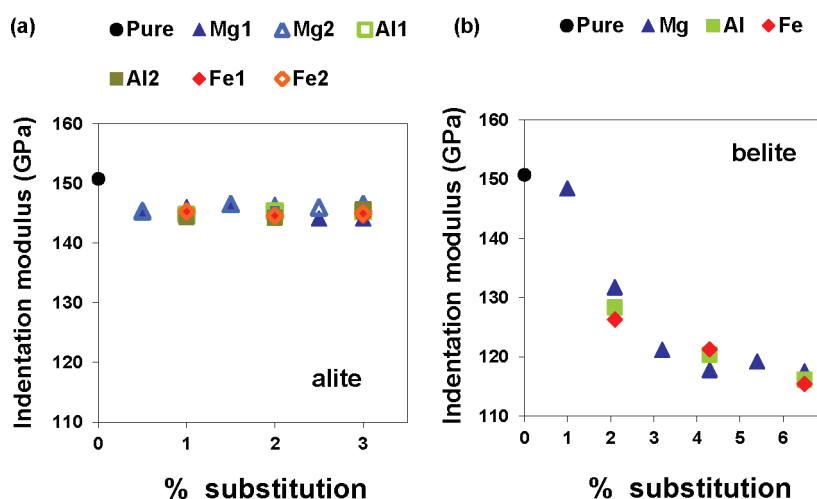
Figure 7. Indentation modulus in GPa of alite (a) and belite (b) as a function of the substitution percentage for the Mg, Al and Fe chemical incorporation.

decreases as impurities are present. It can be seen also that the substitutions have similar effects in both clinker phases, independently of the guest ion. In alite the slight decrease of about 4% is in good agreement with nanoindentation experiments, which reported a decrease of just 6%.[51] According to the same work,[51] belite elastic properties are even less affected by chemical impurities, although our results show the opposite trend. The decrease in the belite indentation modulus is ∼15%, more pronounced than in alite. In view of the chemical structure, this could be related to the lower flexibility of belite. As we have mentioned before, the structure of belite is less flexible than alite because of the absence of free or pure ionic oxygen atoms. The incorporation of guest ions has, hence, a larger impact on the structure, as the rearrangement cannot be so strong. A second argument can be made by analyzing the nature of the chemical bonding. The covalent character of a Si−O bond makes it stronger than an ionic Ca−O. Each defect in belite affects directly the covalent oxygen atoms, disturbing the strong covalent bond. For alite, the chemical incorporations disturb partially covalent bonds and partially ionic bonds, with less effect in the elastic properties. The disagreement between theory and experiment raises an important discrepancy that should be further investigated by higher level ab initio simulations and more detailed experimental measurements.

Electronic Structure. Finally, we discuss the effects of chemical impurities on the electronic structure of these materials. Our force field calculations demonstrate that there is no preferential substitution site, so random alite and belite snapshots were taken for the DFT calculations, with defects close and far to one another for the three chemical substitutions discussed above. We calculate and plot the valence band maximum (VBM) and conduction band minimum (CBM) of alite and belite, which characterize respectively the regions of space where electrons will be depleted and accepted more easily. In other words, the VBM provides an indication of the reactive areas under electrophilic attack, and the CBM the reactive areas under nucleophilic attack. Further details of these calculations are given in the Supporting Information. Here, we focus on the effect of the impurities in the VBM and CBM due to the incorporation of the guest ions, and we support our discussion with a general example in figure 8.
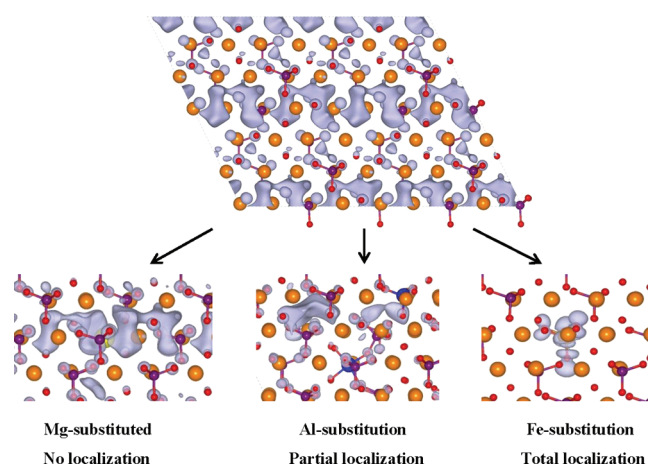

Figure 8. VBM distribution on pure alite unit cell and details of the localization for Mg, Al and Fe chemical substitutions. Detailed pictures of the CBM and VBM within the unit cell of alite and belite with the three studied chemical impurities are given in the Supporting Information.

As can be seen in Figure 8, when Mg^{2+} atoms substitute Ca^{2+}, both the VBM and CBM remain basically unaltered. There is a slight localization around the guest ion, without a significant effect on other points within the unit cell. The calcium and magnesium are isovalent and therefore this substitution does not have a large impact on the reactivity, as was also found experimentally.[21,22] On the other hand, aluminum and iron are aliovalent substitutions, and have a larger impact on the reactive areas. It can be seen that the presence of Al^{3+} localizes both the VBM and CBM of alite. This localization means that the reactivity of some areas is enhanced at the expense of reducing the reactivity of others, decreasing the number of reactive sites. The presence of aluminum partially localizes the VBM and CBM in certain points, but at the same time the new reactive points, the oxygen atoms from aluminate groups, are weakly bonded to the structure. Both effects might balance each other, which could explain why experimentally aluminum substituted alite has the same reactivity or even slightly higher.[21,22] In the iron case, the

reactive regions are highly localized near the defect positions and the Fe−O bond is strong, which helps to explain why the presence of iron reduces the dissolution rate of alite.[21,22] The same behavior discussed for alite was found in belite, as can be seen in the Supporting Information. The presence of magnesium does not change substantially the location of the VBM and CBM, while aluminum partially localizes them and iron completely locates the reactive regions around itself. Therefore, the same dissolution scheme should be expected, with Mg and Al not changing the reaction rate, while iron decreasing it significantly, in good agreement with the trends found in experimental studies.[29]

As noted earlier, several snapshots were simulated by DFT, with substitutions close or far to another and different amounts of impurities. In all cases our results show the same effect on the VBM and CBM. Additionally, it can be argued that the reactivity of a solid depends on the surface electronic structure rather than the bulk. However, it has been stated in previous works that in the case of regular surfaces the CBM and VBM are located in the same sites, just enhanced by surface effects.[52] We can expect then that the conclusions drawn here are extensible to surfaces, at least in absence of low coordinated surfaces like terraces or corners.

CONCLUSIONS

In the present paper we studied by a combination of Force Field and DFT atomistic simulations the impact of chemical impurities (Mg^{2+}, Al^{3+}, and Fe^{3+}) in the structure and properties of the clinker phases alite a belite. The aim was to understand the changes induced by the guest ions right down at the atomic scale, and gain the necessary understanding to modify the materials production at the macroscale and improve their properties. The power of the approach relies in the enormous control on the atomic structure and the great detail of the results, out of the resolution of experimental techniques.

Our simulations show that any crystallographic site within the unit cell is equally probable for the incorporation of Mg^{2+}, Al^{3+}, and Fe^{3+}, and that there is not an optimal distance between guest ions when multiple incorporations take place. There is an important rearrangement of the silicate group orientation and calcium coordination polyhedra to accommodate the defects, as was already stated by experimental works. Despite the change in orientation, the internal structure of the SiO_4^{4-} groups is kept unaltered, while the change occurs in the more flexible Ca−O distances. We found that belite tighter structure makes it more susceptible to structural changes when guest ions are incorporated, and its elastic properties are more affected. Regarding the reactivity, our density functional theory calculations reveal that the reactive areas under nucleophilic and electrophilic attack change differently depending on the guest ion, although they have the same effect on alite and belite. While Mg^{2+} incorporation does not change the electronic structure appreciably, Al^{3+} and Fe^{3+} do, reducing the number of reactive sites. Aluminum however, creates week Al−O bonds highly reactive, balancing the reduction of dissolution points. Opposite, iron dramatically decreases the reactive sites, plus introduces a strong Fe−O bond. This difference might induce a noticeable decrease on the dissolution rate with respect to the pure or the Mg and Al substituted alite and belite.

For the first time, we have insight of a worldwide used material as cement clinker right from the atomic scale. Of special interest is the reactivity of these phases, a key point for cement industry.

Increasing the reactivity of belite will eventually reduce the energy necessary for cement production, reducing its environmental footprint. Our results let us explain observations just empirically so far. Moreover, based on the comparison between experiments and theory, we have the opportunity to predict the effect of new guest ions in the clinker structure and properties.

ASSOCIATED CONTENT

S **Supporting Information.** Detailed information of the force field potentials and parameters, figures of alite and belite silicate tetrahedral reorientation, detailed graphics of alite and belite lattice parameters for all the chemical substitutions and substitution percentage, and figures of alite and belite conduction band maximum (CBM) and valence band minimum (VBM) for all the chemical substitutions. This material is available free of charge via the Internet at http://pubs.acs.org.

AUTHOR INFORMATION

Corresponding Author
*E-mail: hmanzano@mit.edu (H.M); edurgun@mit.edu (E.D.).

ACKNOWLEDGMENT

REFERENCES

(1) Lea, F. M.; Hewlett, P. C. *Lea's Chemistry of Cement and Concrete*,. 4th ed.; Elsevier Butterworth-Heinemann: Oxford, U.K., 1998; p 1053.

(2) Welch, J. H.; Gutt, W. *J. Am. Ceram. Soc.* **1959**, *42* (1), 11–15.

(3) Cuberos, A. J. M.; De la Torre, A. G.; Alvarez-Pinazo, G.; Martin-Sedeno, M. C.; Schollbach, K.; Pollmann, H.; Aranda, M. A. G. *Environ. Sci. Technol.* **2010**, *44* (17), 6855–6862.

(4) Martin-Sedeno, M. C.; Cuberos, A. J. M.; De la Torre, A. G.; Alvarez-Pinazo, G.; Ordonez, L. M.; Gateshki, M.; Aranda, M. A. G. *Cem. Concr. Res.* **2010**, *40* (3), 359–369.

(5) De la Torre, A. G.; Morsli, K.; Zahir, M.; Aranda, M. A. G. *J. Appl. Crystallogr.* **2007**, *40*, 999–1007.

(6) Li, G. S.; Gartner, G. M. High-belite sulfoaluminate clinker: fabrication process and binder preparation. French patent application 04-51586 (Publication 2873366), 27/01/2006, 2006.

(7) Chromy, S.; Maki, I. *Cem. Concr. Res.* **1982**, *12* (4), 511–516.

(8) Maki, I.; Chromy, S. *Cem. Concr. Res.* **1978**, *8* (4), 407–414.

(9) Taylor, H. F. *Cement Chemistry*, 2 ed.; Thomas Telford Publishing: London, 1997.

(10) Henderson, D. M.; Gutowsky, H. S. *Am. Mineral.* **1962**, *47* (11−12), 1231–1251.

(11) Maki, I. In *Relationship of Processing Parameters to Clinker Properties; Influence of Minor Components*, 8th International Congress on the Chemistry of Cement, Rio de Janeiro; Abla Grafica e Editora Ltda.: Rio de Janeiro, 1986; pp 34−47.

(12) Moranville-Regourd, M.; Boikova, A. I. In *Chemistry, Structure, Properties and Quality of Clinker*, 9th International Congress on the Chemistry of Cement, New Delhi; National Council for Cement and Building Materials: New Delhi, 1992; pp 23−45.

(13) Nishi, F.; Takeuchi, Y.; Maki, I. *Z. Kristallogr.* **1985**, *172* (3−4), 297–314.

(14) Bigare, M.; Guinier, A.; Mazieres, C.; Regourd, M.; Yannaqui., N; Eysel, W.; Hahn, T.; Woermann, E. *J. Am. Ceram. Soc.* **1967**, *50* (11), 609–&.

H

dx.doi.org/10.1021/cg200212c |*Cryst. Growth Des.* XXXX, XXX, 000–000

(15) Regourd, M. *C. R. Hebd. Seances Acad. Sci., Ser. B* **1979**, *289* (1), 17–20.

(16) Dunstetter, F.; de Noirfontaine, M. N.; Courtial, M. *Cem. Concr. Res.* **2006**, *36* (1), 39–53.

(17) Mumme, W. G. *Neues Jahrb. Mineral., Monatsh.* **1995**, *4*, 145–160.

(18) Woermann, E.; Hahn, T.; Eysel, W. *Cem. Concr. Res.* **1979**, *9* (6), 701–711.

(19) Maki, I.; Goto, K. *Cem. Concr. Res.* **1982**, *12* (3), 301–308.

(20) Maki, I.; Kato, K. *Cem. Concr. Res.* **1982**, *12* (1), 93–100.

(21) Stephan, D.; Wistuba, S. *J. Eur. Ceram. Soc.* **2006**, *26* (1−2), 141–148.

(22) Valenti, G. L.; Sabatelli, V.; Marchese, B. *Cem. Concr. Res.* **1978**, *8* (1), 61–72.

(23) Barbier, J.; Hyde, B. G. *Acta Crystallographica Section B-Structural Science* **1985**, *41* (DEC), 383–390.

(24) Feng, X. J.; Min, X. M.; Tao, C. X. *Cem. Concr. Res.* **1994**, *24* (7), 1311–1316.

(25) Smith, D. K.; Majumdar., A; Ordway, F. *Acta Crystallogr.* **1965**, *18*, 787–&.

(26) Jost, K. H.; Ziemer, B.; Seydel, R. *Acta Crystallogr., Sect. B* **1977**, *33* (JUN15), 1696–1700.

(27) Hudson, K. E.; Groves, G. W. *Cem. Concr. Res.* **1982**, *12* (1), 61–68.

(28) ElDidamony, H.; Sharara, A. M.; Helmy, I. M.; ElAleem, S. A. *Cem. Concr. Res.* **1996**, *26* (8), 1179–1187.

(29) Kim, Y. M.; Hong, S. H. *J. Am. Ceram. Soc.* **2004**, *87* (5), 900–905.

(30) Mumme, W. G.; Hill, R. J.; Bushnellwye, G.; Segnit, E. R. *Neues Jahrb. Mineral., Abh.* **1995**, *169* (1), 35–68.

(31) Darntoft, J. S.; Lukasik, J.; Herfort, D.; Sorrentino, D.; Gartner, E. M. *Cem. Concr. Res.* **2008**, *38* (2), 115–127.

(32) Kantro, D. L.; Weise, C. H. *J. Am. Ceram. Soc.* **1979**, *62* (11−1), 621–626.

(33) Karakasidis, T. E.; Charitidis, C. A. *Mater. Sci. Eng. C* **2007**, *27*, 1082–1089.

(34) Manzano, H.; Dolado, J. S.; Ayuela, A. *J. Am. Ceram. Soc.* **2009**, *92* (4), 897–902.

(35) Manzano, H.; Dolado, J. S.; Ayuela, A. *Acta Mater.* **2009**, *57* (5), 1666–1674.

(36) Manzano, H.; Gonzalez-Teresa, R.; Dolado, J. S.; Ayuela, A. *Mater. Constr.* **2010**, *60* (299), 7–19.

(37) Zacate, M. O.; Grimes, R. W. *Philos. Mag. A* **2000**, *80* (4), 797–807.

(38) Gale, J. D. *J. Chem. Soc., Faraday Trans.* **1997**, *93* (4), 629–637.

(39) Gale, J. D.; Rohl, A. L. *Mol. Simul.* **2003**, *29* (5), 291–341.

(40) Ewald, P. P. *Ann. Phys.* **1921**, *64* (3), 253–287.

(41) Shannon, D. F. *Math. Comput* **1970**, *24*, 647–656.

(42) Leach, A. R. *Molecular Modelling: Principles and Applications*, 2nd ed.; Prentice Hall: Harlow, England, 2001; p xxiv, 744 p., [16] p. of plates.

(43) Sun, G. Y.; Kurti, J.; Rajczy, P.; Kertesz, M.; Hafner, J.; Kresse, G. *THEOCHEM* **2003**, *624*, 37–45.

(44) Blochl, P. E. *Phys. Rev. B* **1994**, *50* (24), 17953–17979.

(45) Perdew, J. P.; Burke, K.; Ernzerhof, M. *Phys. Rev. Lett.* **1996**, *77* (18), 3865–3868.

(46) Jansang, B.; Nonat, A.; Skibsted, J. In *Modelling of Guest−Ion Incorporation in the Anhydrous Calcium Silicate Phases of Portland Cement by Periodic Density Functional Theory Calculations* ConMod 2010; EPFL: Switzerland, 2010.

(47) De La Torre, A. G.; Bruque, S.; Campo, J.; Aranda, M. A. G. *Cem. Concr. Res.* **2002**, *32* (9), 1347–1356.

(48) Takeuchi, Y.; Nishi, F.; Maki, I. *Acta Crystallogr. A* **1984**, *40*, C215–C216.

(49) De la Torre, A. G.; De Vera, R. N.; Cuberos, A. J. M.; Aranda, M. A. G. *Cem. Concr. Res.* **2008**, *38* (11), 1261–1269.

(50) Porras-Vazquez, J. M.; De la Torre, A. G.; Losilla, E. R.; Aranda, M. A. G. *Solid State Ionics* **2007**, *178* (15−18), 1073–1080.

(51) Velez, K.; Maximilien, S.; Damidot, D.; Fantozzi, G.; Sorrentino, F. *Cem. Concr. Res.* **2001**, *31* (4), 555–561.

(52) Cárdenas, C.; Proft, F. D.; Chamorro, E.; Fuentealba, P.; P., G. *J. Phys. Chem.* **2008**, *128*, 034708–034715.